The FEBS Journal

FEBS PRESS science publishing by scientists

Necroptosis directly induces the release of full-length biologically active IL-33 *in vitro* and in an inflammatory disease model

Inbar Shlomovitz[1], Ziv Erlich[1], Mary Speir[2,3], Sefi Zargarian[1], Noam Baram[1], Maya Engler[1], Liat Edry-Botzer[1], Ariel Munitz[1], Ben A. Croker[2,3] and Motti Gerlic[1]

1 Department of Clinical Microbiology and Immunology, Sackler Faculty of Medicine, Tel Aviv University, Israel
2 Division of Hematology/Oncology, Boston Children's Hospital, MA, USA
3 Department of Pediatrics, Harvard Medical School, Boston, MA, USA

Keywords
cell death; DAMP; IL-33; MLKL; necroptosis

Correspondence
M. Gerlic and I. Shlomovitz, Department of Clinical Microbiology and Immunology, Sackler Faculty of Medicine, Tel Aviv University, Tel Aviv 69978, Israel
Tel: +972-36409069
E-mails: mgerlic@post.tau.ac.il (MG); shlomovitz1@mail.tau.ac.il (IS)

(Received 11 September 2018, revised 10 November 2018, accepted 18 December 2018)

doi:10.1111/febs.14738

Interleukin-33 (IL-33) is a pro-inflammatory cytokine that plays a significant role in inflammatory diseases by activating immune cells to induce type 2 immune responses upon its release. Although IL-33 is known to be released during tissue damage, its exact release mechanism is not yet fully understood. Previously, we have shown that cleaved IL-33 can be detected in the plasma and epithelium of *Ripk1*$^{-/-}$ neonates, which succumb to systemic inflammation driven by spontaneous receptor-interacting protein kinase-3 (RIPK3)-dependent necroptotic cell death, shortly after birth. Thus, we hypothesized that necroptosis, a RIPK3/mixed lineage kinase-like protein (MLKL)-dependent, caspase-independent cell death pathway controls IL-33 release. Here, we show that necroptosis directly induces the release of nuclear IL-33 in its full-length form. Unlike the necroptosis executioner protein, MLKL, which was released in its active phosphorylated form in extracellular vesicles, IL-33 was released directly into the supernatant. Importantly, full-length IL-33 released in response to necroptosis was found to be bioactive, as it was able to activate basophils and eosinophils. Finally, the human and murine necroptosis inhibitor, GW806742X, blocked necroptosis and IL-33 release *in vitro* and reduced eosinophilia in *Aspergillus fumigatus* extract-induced asthma *in vivo*, an allergic inflammation model that is highly dependent on IL-33. Collectively, these data establish for the first time, necroptosis as a direct mechanism for IL-33 release, a finding that may have major implications in type 2 immune responses.

Abbreviations

Asp., *Aspergillus fumigatus* extract; AZD 5582, 3,3′-[2,4-Hexadiyne-1,6-diylbis[oxy[(1S,2R)-2,3-dihydro-1H-indene-2,1 diyl]]]bis[*N*-methyl-L-alanyl-(2S)-2-cyclohexylglycyl-L-prolinamide; BAL, bronchoalveolar lavage; CC3, cleaved caspase-3; COPD, chronic obstructive pulmonary disease; DAMP, danger-associated molecular patterns; DMEM, Dulbecco's modification of Eagle; ECV, extracellular vesicles; GSK'872, GSK2399872A; GW80, GW806742X; H&E, hematoxylin and eosin; HRP, horseradish peroxidase; IL, interleukin; IP, intraperitoneal injection; MBP, major basic protein; MLKL, mixed lineage kinase-like protein; Nec-1s, necrostatin-1s; NSA, necrosulfonamide; PI, propidium iodide; pMLKL, phosphorylated MLKL; RIPK1, receptor-interacting protein kinase-1; RIPK3, receptor-interacting protein kinase-3; SD, standard deviation; S/N, supernatant; SMAC, second mitochondrial-derived activator of caspases; sST2, soluble ST2; TLR, Toll-like receptors; TNF-α, tumor necrosis factor-α; TS, TNF-α and SMAC; TSZ, TNF-α, SMAC, and Z-VAD-fmk; Z-VAD-fmk, carbobenzoxy-valyl-alanyl-aspartyl-[*O*-methyl]- fluoromethylketone.

Introduction

Interleukin-33 (IL-33), a pro-inflammatory cytokine belonging to the IL-1 superfamily [1], is expressed in epithelial cells exposed to the environment, such as in the skin, the gut, and respiratory tract, as well as in endothelial cells and fibroblasts [2,3]. The N-terminal region of IL-33 contains a nuclear binding domain, hence its constitutive expression is in the nuclei of these cells, where it binds to the histone heterodimer H2A-H2B at the nucleosome surface [4]. The nuclear function of IL-33 is still a matter of debate and it was recently shown to have no effect on global gene expression in an IL-33-stably expressing esophageal epithelial cell line [5]. Upon binding to its surface receptor, ST2, IL-33 signals via myeloid differentiation primary response 88 to activate NF-κB and mitogen-activated protein kinases. This consequently promotes type 2 cytokine secretion and the survival and proliferation of $ST2^+$ myeloid cells, such as eosinophils, basophils, and mast cell, as well as lymphoid cells, including Tregs, T_H2 cells, and type 2 innate lymphoid cells [6]. Transgenic (tg) mice lacking the N-terminal nuclear domain of IL-33 have elevated serum IL-33 levels and ST2-dependent lethal inflammation, highlighting the potency of extracellular IL-33 and the importance of its nuclear sequestration at baseline [7].

Unlike other IL-1 family members, full-length IL-33 is biologically active but is tightly regulated at several cleavage sites. The apoptotic caspases, caspase-3 and caspase-7, process IL-33 to an inactive product by cleaving its C-terminal IL-1-like domain (112–270). The inflammatory caspases, caspase-1, -4, and -5, hardly possess this ability [8,9]. Shown biochemically, cleavage by neutrophil- [10] and mast cell- [11] proteases, such as neutrophil elastase, cathepsin G, chymase, and tryptase, results in an IL-33 hyperactive form. However, supernatant (S/N) containing granule proteases from activated neutrophils was recently shown to suppress IL-33 activity overall, as cleavage by proteinase 3 opposes cathepsin G and elastase-mediated hyperactivation [12]. Proteases from environmental allergens can also cleave IL-33 into mature products that exhibit increased potency *in vitro* and *in vivo* [13]. Lastly, IL-33 can undergo additional regulatory extracellular modification by cysteine oxidation [14] or by binding to its decoy receptor, soluble ST2 (sST2) [15], that abolishes its activity.

Interleukin-33 is a crucial actor in lung inflammation. sST2 and IL-33 levels in serum and induced sputum are higher in young asthmatic patients compared with healthy controls [16,17], as well as in chronic obstructive pulmonary disease (COPD) patients [18]. IL-33 and its receptor are identified as major susceptibility loci for asthma in several genome-wide association studies [19]. IL-33-deficient mice studies emphasize the essential role of IL-33 in inducing IL-13, mucus overproduction [1,20], and lung disease following viral infection [21]. When administered directly to mouse lung, cleaved IL-33 induces eosinophilic inflammation and airway hyperresponsiveness [22,23].

Because IL-33 lacks a secretion signal sequence, its release mechanism remains unknown. *In vitro*, IL-33 was shown to be released from endothelial cells following freeze-thaw cycles and exposure to nonionic detergents, such as Nonidet P-40 and Triton X-100 [9]. Endogenous IL-33 was released from THP-1 cells, bone marrow-derived macrophages and bone marrow dendritic cells upon exposure to hydrogen peroxide, sodium azide, streptolysin O, and high doses of daunorubicin, while hardly secreted upon apoptosis induction [8]. IL-33 was detected in the S/N of fibroblast-like synoviocytes from rheumatoid arthritis patients cultured with IL-1β and tumor necrosis factor-α (TNF-α) and treated with Nonidet P-40 [24]. IL-33 chromatin binding was recently reported to slow release during cryoshock- or calcium ionophore A23187-induced necrosis in an esophageal epithelial cell line [5]. Alum-induced cellular necrosis results in elevated levels of IL-33 following intraperitoneal injection (IP) *in vivo* [25]. In addition, IL-33 is released from cultured endothelial cells following scraping, which mimics mechanical forces *in vivo* [9]. Biomechanical stress by biaxial stretch induces IL-33 secretion from IL-33-stably expressing fibroblasts and primary human skin fibroblasts [26]. All together, these experiments suggest that IL-33 may be released upon accidental cell death (necrosis).

Necroptosis, which was originally defined as a receptor-interacting protein kinase 1 (RIPK1)-dependent and caspase-independent form of cell death [27], was later discovered to require RIPK3 and the mixed lineage kinase-domain like pseudokinase MLKL [28–30]. Hence, necroptosis is best defined as RIPK3/MLKL-dependent, caspase-independent, inflammatory cell death [31]. While various stimuli can activate necroptosis by engaging death receptors, Toll-like receptors (TLRs) or intracellular receptors, they all require caspase-8 inhibition to prevent cleavage and inactivation of RIPK3 [32–34]. When caspase-8 activity is blocked by different viral or bacterial pathogens, or spontaneously in specific settings, extra- or intracellular signals trigger phosphorylation of RIPK3, which leads to aggregation of MLKL and its phosphorylation by RIPK3 [28,35–37]. Phosphorylated MLKL (pMLKL) then translocates to the plasma membrane and compromises its integrity,

inducing necroptosis [38–40]. Thus, necroptosis can be prevented by genetic depletion of RIPK3 and MLKL, or chemically inhibited by necrostatin-1s (Nec-1s) [41,42], GSK2399872A (GSK'872) [30], and necrosulfonamide (NSA) [37] or GW806742X (GW80) [43], which inhibit RIPK1, RIPK3, and MLKL, respectively. Unlike apoptosis, necroptosis is characterized by cell swelling, membrane permeabilization and a leakage of cytoplasmic content resulting in the release of danger-associated molecular patterns (DAMPs) that may act as alarmins to induce inflammation [31,44–46]. Cleaved IL-33, which was detected in the plasma of mice lacking RIPK1, was suggested to be one such alarmin. *Ripk1*$^{-/-}$ mice undergo spontaneous apoptosis and necroptosis and die at birth due to systemic inflammation. However, extracellular IL-33 is still found in the skin and plasma of *Ripk1*$^{-/-}$*Casp8*$^{-/-}$ mice, which, although protected from apoptotic cell death, still die from lethal inflammation. On the other hand, *Ripk1*$^{-/-}$*Ripk3*$^{-/-}$ or *Ripk1*$^{-/-}$*Mlkl*$^{-/-}$ mice, which are protected from necroptosis, do not release IL-33, suggesting necroptosis as a potential release mechanism for bioactive IL-33 [44].

Many features of IL-33 biology make it an important alarmin for further study: the poorly defined release mechanism, the unique nuclear localization in barrier tissues, its suppression by apoptosis and conversely release in response to trauma and its multiple cleavage sites controlling its extracellular activity. Here, we aimed to define the direct role of necroptosis in IL-33 release. We show that full-length and, importantly, bioactive IL-33 is released directly from necroptotic, but not apoptotic, cells. We report that the necroptosis inhibitor GW80 inhibits necroptosis and IL-33 release *in vitro* and attenuates lung inflammation *in vivo* in an IL-33-dependent *Aspergillus fumigatus* extract-induced asthma model. Thus, we propose that necroptosis is a direct IL-33 release mechanism, implying that IL-33 is a necroptotic DAMP. Furthermore, our *in vivo* results suggest a clear role for necroptotic release of IL-33 in mediating lung pathology in asthma, offering a new avenue for therapeutic intervention.

Results

Necroptosis induces IL-33 release

To investigate the direct role of necroptosis in IL-33 release, we established two *in vitro* systems of stably expressing IL-33-GFP cell lines that are sensitive to both apoptosis and necroptosis: (a) HaCaT – a human keratinocyte cell line; and (b) L929 – a murine fibrosarcoma cell line (Fig. 1A,B). To enable an endogenous IL-33 localization pattern, a self-cleaving peptide (T2A) was inserted between the IL-33 and GFP sequences. Immunofluorescence staining confirmed the nuclear localization of IL-33 in the infected cells, as reported for the endogenous cytokine (Fig. 1C,D) [4,47]. As expected, IL-33-expressing HaCaT cells were sensitive to apoptosis, induced by TNF-α and a second mitochondrial-derived activator of caspases (SMAC) mimetic (TS), and necroptosis, induced by TNF-α, a SMAC mimetic, and the pan-caspase inhibitor carbobenzoxy-valyl-alanyl-aspartyl-[*O*-methyl]- fluoromethylketone (z-VAD-fmk; TSZ; Fig. 2A) [48]. IL-33 was detected in the S/N of necroptotic, but not apoptotic, HaCaT cells in a time-dependent manner following treatment (Fig. 2B,C). L929 cells treated with apoptotic stimuli (TS), are known to present a mixed phenotype of both apoptotic and necroptotic cell death, without the need for exogenous caspase inhibition [49]. In this setting, L929 cells exhibited slower death kinetics (Fig. 2D), without the detection of IL-33 in the S/N (Fig. 2E,F). Necroptosis inhibition by the chemical inhibitors, Nec-1s and NSA, inhibited IL-33 release, confirming necroptosis as the release mechanism (Fig. 2B,C,E,F). These results demonstrate that necroptosis directly induces full-length IL-33 release in both human and murine *in vitro* systems.

We have previously reported that an early stage in necroptotic cell death includes phosphatidylserine exposure and release of extracellular vesicles (ECVs) that contain pMLKL [48]. As pMLKL detection in the necroptotic S/N correlated with IL-33 detection, we decided to examine the possibility that IL-33 is being released in ECVs. However, ECVs separation demonstrated a distinct localization pattern for pMLKL and IL-33. Full-length IL-33 was detected in the soluble fraction of necroptotic cell S/N, while pMLKL was detected in the ECVs fractions 7–9 (Fig. 3).

Necroptotic IL-33 is biologically active

We next investigated whether the IL-33 released by necroptosis is biologically active using two different models based on published systems [11,50]: (a) KU812, a human basophilic cell line, which secretes IL-5 in response to recombinant IL-33 in a dose-dependent manner (Fig. 4A); and (b) primary eosinophils, isolated from the peritoneal fluid of IL-5 tg mice, which secrete IL-6 in response to recombinant IL-33 in a dose-dependent manner (Fig. 4B). Since these cells are being exposed to apoptotic and necroptotic stimuli (e.g., TS and TSZ) left in the S/N from the treated IL-33-expressing cells, we tested their direct sensitivity to these death inducers. KU812 cells and eosinophils demonstrated similar cell death kinetics in response to

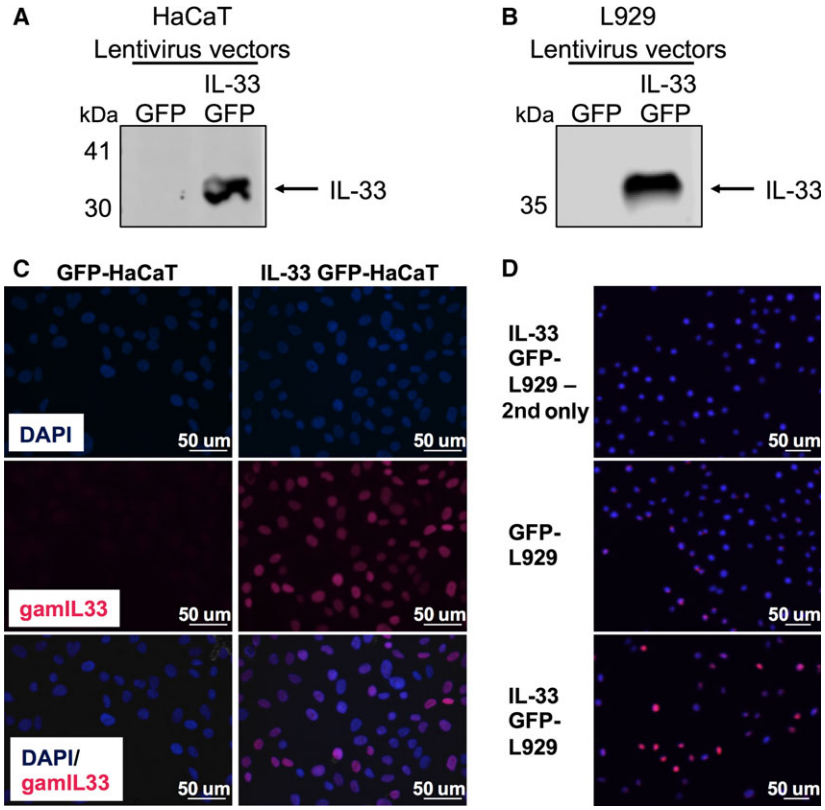

Fig. 1. Nuclear localization of IL-33 in IL-33-GFP-stably expressing cells. (A, B) Immunoblot analysis of IL-33 in lysates from GFP+ sorted HaCaT (A) or L929 (B) cells after transduction with GFP or IL-33 GFP-containing lentivirus vectors. (C, D) Immunofluorescence staining for IL-33 (pink) in GFP or GFP-IL-33-stably expressing HaCaT (C) or L929 (D). 2nd Only – IL-33 GFP L929 cells were stained with anti-goat Alexa Flour 680 without anti IL-33 antibody. Cell nuclei were counterstained with DAPI (blue).

both apoptotic and necroptotic stimuli (Fig. 4C,D). Thus, to control for this direct effect, and for any other DAMPs that may be released during our treatment, we compared the ability of apoptotic and necroptotic IL-33-GFP HaCaT cells to induce IL-5 (KU812) or IL-6 (primary IL-5tg eosinophils) with that of apoptotic and necroptotic GFP-only HaCaT. Following an overnight co-culture, S/Ns were collected and tested for IL-5 or IL-6 as a read-out of IL-33 activity (Fig. 4E). KU812 cells that were co-cultured with IL-33-GFP necroptotic cells secreted significantly higher levels of IL-5 compared to GFP-only necroptotic cells, or IL-33-GFP apoptotic cells (Fig. 4F). Primary IL-5tg eosinophils exhibited a similar pattern for IL-6 release (Fig. 4G). Therefore, we conclude that the full-length IL-33 released during necroptosis retains its biological activity.

GW806742X, a murine MLKL inhibitor, reduces lung eosinophilia in *Aspergillus* extract-induced asthmatic mice

Among patients with persistent asthma requiring specialist referral, 20–25% have a skin-test reactivity to *Aspergillus* or other fungi [51,52]. Asthmatic children with a positive IgE or skin prick test response to *A. fumigatus*, *Alternaria alternata*, or *Cladosporium herbarum*, have an earlier onset of symptoms with higher total IgE and airway IL-33 [53]. Therapeutically, targeting the IL-33 receptor, ST2, significantly reduces

Fig. 2. Full-length IL-33 is released from necroptotic cells. GFP- or IL-33 GFP-expressing HaCaT (A–C) or L929 (D–F) cells were treated with TNF-α (1.15 nM) and SMAC (AZD 5582, 2.5 μM; TS) to induce apoptosis, or with TSZ (20 μM) to induce necroptosis, in the presence, or absence, of necroptosis inhibitors for RIPK1 (Nec-1s, 5 μM), RIPK3 (GSK'872, 5 μM) or MLKL (NSA, 1 μM). (A, D) Cell viability was monitored using PI via real-time imaging (IncucyteZOOM). (B, E) ELISA of IL-33 in the S/N of treated cells at different time points after stimulation. (C, F) Immunoblot analysis of cell lysates and S/N at the indicated time points after stimulation using antibodies against pMLKL and CC3, to confirm necroptosis or apoptosis, respectively, and total MLKL and IL-33. (A, D) Data are presented as the mean of triplicate samples ± SD. (B, E) Each symbol represents an individual triplicate sample. TSZ is significantly different from any other treatment in each time point, $P < 0.0001$. ***$P < 0.001$, ****$P < 0.0001$ for the last time point [two-way ANOVA followed by Tukey's multiple-comparison test (A, B, D, E)]. (C, F) Data are representative of at least three independent experiments.

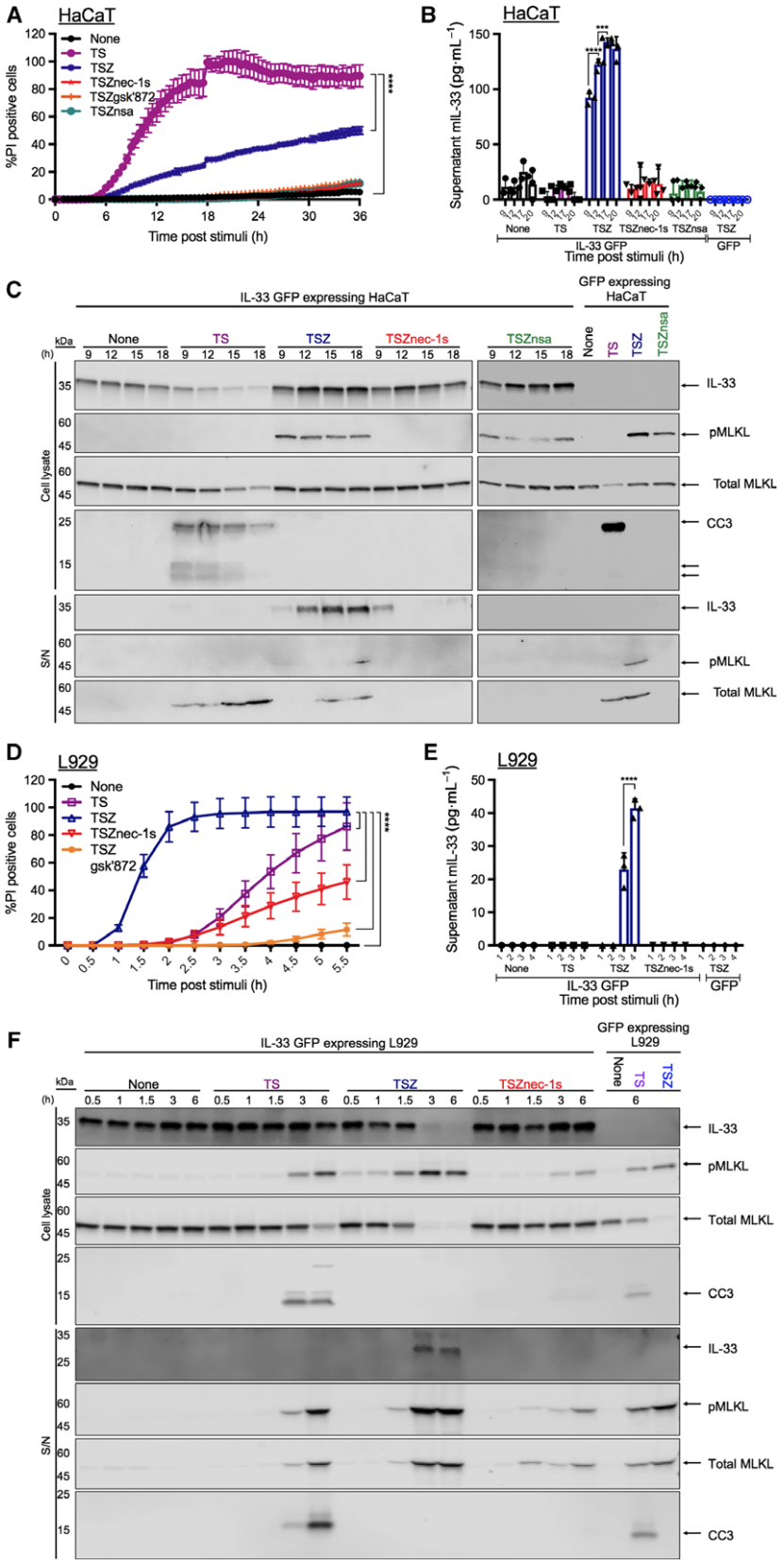
A
HaCaT
None
TS
TSZ
TSZnec-1s
TSZgsk'872
TSZnsa
%PI positive cells
Time post stimuli (h)
B
HaCaT
Supernatant mIL-33 (pg·mL⁻¹)
None
TS
TSZ
TSZnec-1s
TSZnsa
TSZ
IL-33 GFP
GFP
Time post stimuli (h)
C
IL-33 GFP expressing HaCaT
GFP expressing HaCaT
kDa
(h)
Cell lysate
S/N
IL-33
pMLKL
Total MLKL
CC3
D
L929
%PI positive cells
Time post stimuli (h)
E
L929
Supernatant mIL-33 (pg·mL⁻¹)
IL-33 GFP
GFP
Time post stimuli (h)
F
IL-33 GFP expressing L929
GFP expressing L929
Cell lysate
S/N
IL-33
pMLKL
Total MLKL
CC3

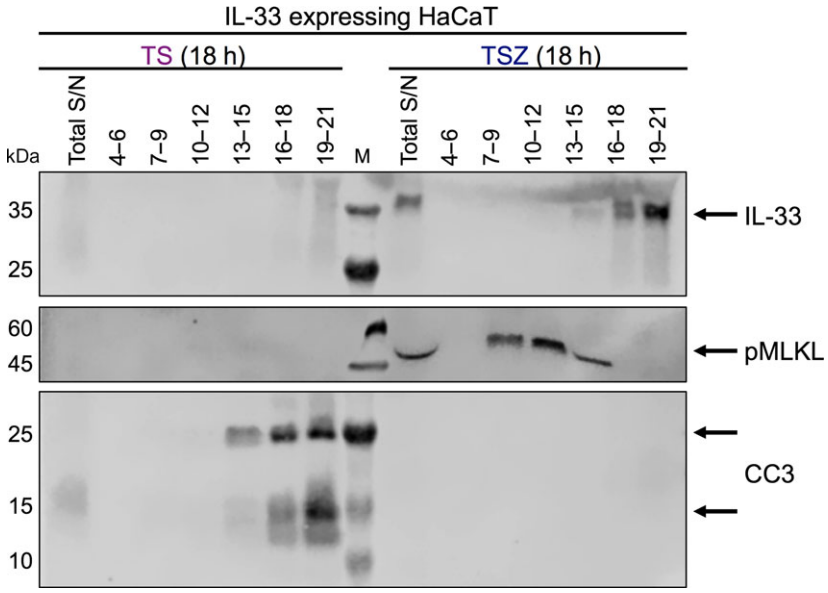

Fig. 3. IL-33 is released during necroptosis in the free protein fraction. HaCaT cells were treated as Fig. 2. Immunoblot analysis of different concentrated isolated fractions (qEV,ZION) from apoptotic or necroptotic HaCaT S/N using antibodies against pMLKL, CC3 and IL-33. Extracellular vesicles are isolated in fractions 7–9, while free proteins are in fractions 13–25. M, protein marker.

airway inflammation, airway remodeling, and hyperactivity in a mouse model of *Aspergillus*-induced asthma [54]. ST2-deficient mice also demonstrate reduced airway hyperactivity in response to Asperamide-B, an *Aspergillus* glycosphingolipid [55].

Our *in vitro* data raised the hypothesis that necroptosis-induced IL-33 release may contribute to the development of allergic airway disease. To this end, we examined the role of necroptosis in an *A. fumigatus* extract (*Asp*.)-induced allergic airway inflammation, using a recently discovered murine necroptosis inhibitor, GW80 [43,56,57]. Treatment with GW80 resulted in delayed cell death kinetics for TSZ-, but not TS-, treated IL-33-GFP-expressing L929 or HaCaT cells, thus confirming its ability to inhibit necroptotic cell death *in vitro* (Fig. 5A,C). In agreement with our earlier results showing necroptotic release of IL-33, GW80 prevented release of pMLKL and IL-33 into the S/N and retained IL-33 in the cell lysate of TSZ-, but not TS-, treated cells (Fig. 5B,D).Finally, mice treated with GW80 1 h prior to *Asp*.-extract challenge exhibited a decrease in recruitment of eosinophils and $CD4^+$ T cells to the bronchoalveolar space, while neutrophil recruitment was not affected (Fig. 6B–E). GW80 treatment also decreased pMLKL in the bronchoalveolar lavage (BAL) fluid as detected by western blot (Fig. 6G). In correlation, low levels of cleaved IL-33 were detected in the BAL fluid of the *Asp*.-challenged mice, supporting our hypothesis (Fig. 6G). Serum IgE levels were lower in the GW80-treated mice (Fig. 6F). In addition, airway inflammation and lung eosinophil infiltration were reduced in response to GW80 treatment (Fig. 6H–K). In summary, the ability of the necroptotic inhibitor GW80 to attenuate pathology in an IL-33-dependent *Asp*.-induced asthma model suggests a role for necroptosis in IL-33 release in asthma. However, future studies will clarify whether necroptosis effects asthma in an IL-33-dependant or independent manner.

Discussion

Interleukin-33 plays an important role in various inflammatory diseases, such as asthma, allergic skin diseases, obesity, inflammatory bowel diseases, arthritis, myocardial infarction, infections, and cancer [58]. Inhibition of disease in ST2-deficient mice and in mice treated with IL-33-neutralizing antibodies emphasizes that this cytokine has an important extracellular role following its release. In addition, numerous modifications can regulate full-length IL-33 in the extracellular environment to modify its bioactivity. These modifications include oxidation, cleavage, and rapid degradation following cleavage [13]. Yet, the mechanisms for IL-33 release in physiological and pathological environment are poorly understood [59].

Herein, we elucidate, for the first time to our knowledge, the direct role of necroptosis in IL-33 release. We show that full-length, bioactive IL-33 is released during necroptotic, but not apoptotic, cell death. These findings distinguish this necroptotic release from the apoptotic modification, in which IL-33 is cleaved intracellularly by apoptotic caspases to an inactive product [8]. Altogether, these data support a model where IL-33, similar to the other nuclear IL-1 family

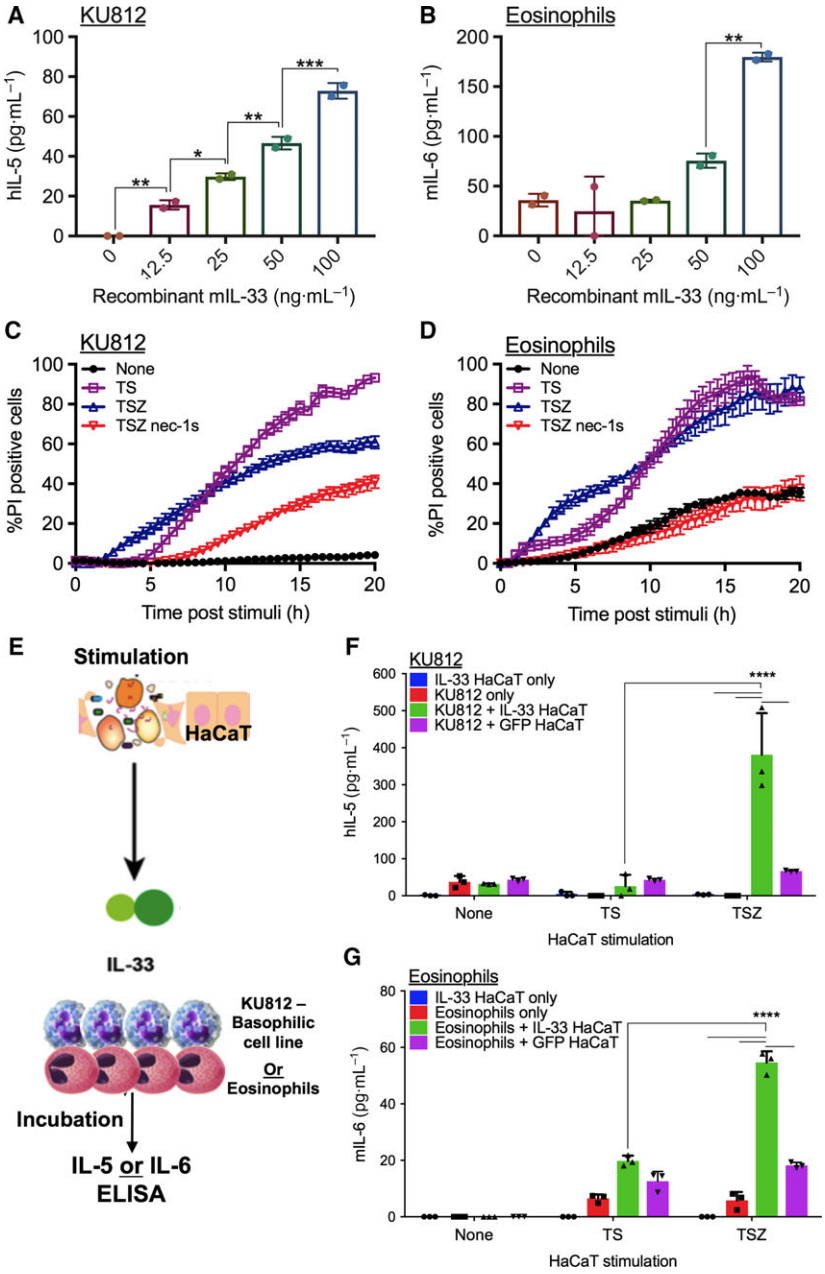

Fig. 4. Necroptotic-released IL-33 activates KU812 cells and eosinophils. (A) ELISA of IL-5 in the S/N of KU812 cells after overnight treatment with various doses of recombinant murine IL-33 to assess activation. (B) ELISA of IL-6 in S/N of eosinophils after overnight treatment with various doses of recombinant murine IL-33 to assess activation. Eosinophils were enriched using negative selection of $B220^{-}$, $CD90.2^{-}$ cells from peritoneal fluid from IL-5 tg mice using magnetic beads (Dynabeads). (C, D) KU812 cells (C) or eosinophils (D) were treated with TS to induce apoptosis, or with TSZ to induce necroptosis, in the presence, or absence, of a RIPK1 inhibitor (Nec-1s). Cell viability was monitored with PI using real-time imaging (IncucyteZOOM). (E) Schematic overview of bioactivity assay. IL-33-GFP- or GFP-expressing HaCaT cells were treated with apoptotic (TS) or necroptotic (TSZ) stimuli for 6 or 16 h before the addition of KU812, a human basophilic cell line (F), or eosinophils (G) for further 24 h. (F) ELISA of IL-5 in S/N of KU812 and HaCaT co-culture. (G) ELISA of IL-6 in S/N of eosinophils and HaCaT co-culture. (A, B) Each symbol represents an individual duplicate sample. $*P < 0.05$, $**P < 0.01$, $***P < 0.001$ (one-way ANOVA followed by Tukey's multiple-comparison test). (C, D) Data are presented as mean of triplicate samples ± SD. (F, G) Each symbol represents an individual triplicate sample. $****P < 0.0001$ (two-way ANOVA followed by Tukey's multiple- comparison test). Data are representative of three independent experiments.

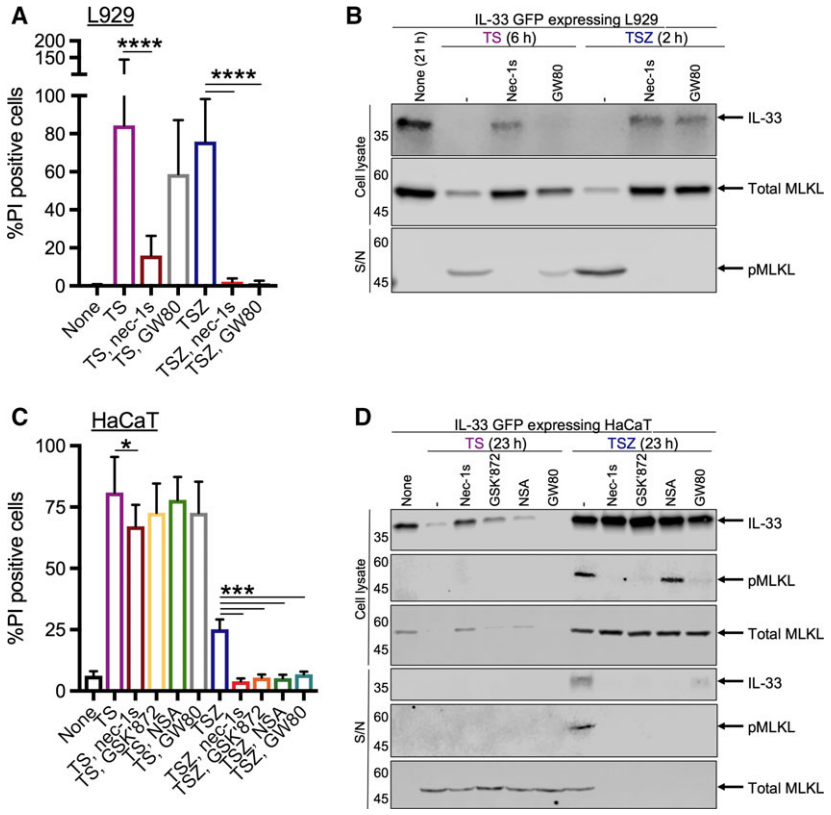

Fig. 5. GW806742X inhibits necroptosis and IL-33 release *in vitro*. IL-33-GFP-expressing L929 (A, B) or HaCaT (C, D) cells were treated with cell death stimuli in the presence, or absence, of necroptosis inhibitors for RIPK1 (Nec-1s, 5 μM), RIPK3 (GSK'872, 5 μM), human MLKL translocation (NSA, 1 μM) or MLKL (GW80, 0.3 μM). (A, C) Cell viability was monitored with PI using real-time imaging (IncucyteZOOM).(B, D) Immunoblot analysis of cell lysates and S/N at indicated time points after stimulation using antibodies against pMLKL to confirm necroptosis, total MLKL, and IL-33. (A, C) Data are presented as mean of nine images per treatment ± SD. $*P < 0.05$, $***P < 0.001$, $****P < 0.0001$ (two-way ANOVA followed by Tukey's multiple-comparison test). (B) Data are representative of least two independent experiments.

members, functions as a canonical DAMP at the intersection of cell death and inflammation [60].

Il33 mRNA encodes a protein of 270 residues in human and 266 residues in mouse, with mass of 30 and 29.9 kDa, respectively. The human gene is located on chromosome 9p24.1, while the murine gene is found on the syntenic chromosome 19qC1. Human and mouse IL-33 are 55% identical at the amino acid level, and are both the closet relatives of IL-18 of all IL-1 family members [1]. The human and murine genes share similar organization with seven exons which are highly conserved by size. Alignment of these two proteins revealed that they are both composed of two evolutionary conserved regions separated by different linker region, one of which is the chromatin binding motif in the N-terminal domain [61]. Crystal structure studies revealed that the surface charge complementarity between IL-33 and its receptor, ST2, is critical for specific binding [62]. Murine lymphoid cells are being as effectively activated by recombinant human IL-33 as by the recombinant mouse IL-33 [58]. Here, for the first time to our knowledge, we presented the complementary phenomenon, in which the mouse IL-33 activates human basophils. Of note, mouse IL-33 was found to undergo a rapid degradation following cleavage while the human cleaved product remains stable [13].

Fig. 6. GW806742X reduces BAL fluid pMLKL and eosinophilia in *Asp.*-induced asthmatic mice. C57BL/6J-RccHsd wild-type female, 6- to 7-week-old mice were sensitized IP with 20 μg of *Asp.* mixed with Alum on days 0 and 7, and then challenged IN with 10 μg *Asp.* on days 18,19, and 20. Control mice were treated with saline (PBS). Mice were sacrificed and analyzed on day 21. Where indicated, GW806742X, a necroptosis inhibitor (100 μM in 50 μL) was administrated IN 1-h prior to *Asp.* challenge. (A) Schematic overview of the model. (B–E) Flow cytometry analysis of the frequency of eosinophils (B), alveolar macrophages (C), neutrophils (D), $CD4^+$ T cells (E) in the BAL fluid of treated mice (Attune NxT). (F) ELISA of serum IgE of treated mice. (G) Immunoblot analysis of BAL fluid of treated mice using antibodies against pMLKL, total MLKL and IL-33. (H, J) Lungs were stained with H&E and were evaluated for peribronchial inflammation in 10× magnification by 1–5 scoring by two independent researchers. Arrows point to cellular infiltration; arrowheads point to mucus. (I, K) Immunohistochemical analysis of MBP positive cells (eosinophils). (J, K) Representative lung tissue sections. (B–F) Each symbol represents an individual mouse from two independent experiments ± SD. $*P < 0.05$, $**P < 0.01$ (Mann–Whitney test). (H) Each symbol represents the mean of two scores for triplicate peribronchial fields for each individual mouse ± SD. (I) Each symbol represents the mean of MBP-positive cells per field in ten randomly selected fields from each lung, as measured via IMAGEJ ± SD. $**P < 0.01$, $***P < 0.001$ [Mann–Whitney test (H, I)]. IN, intranasal injection.

It should be noted that another mechanism for IL-33 release has been reported. Human tracheobronchial epithelial cells cultured from COPD patients [18], as well as corneal epithelial cells [63], astrocytes, and glial cells [64], stimulated with TLR ligands were shown to release IL-33 via an ATP-dependent, noncytotoxic

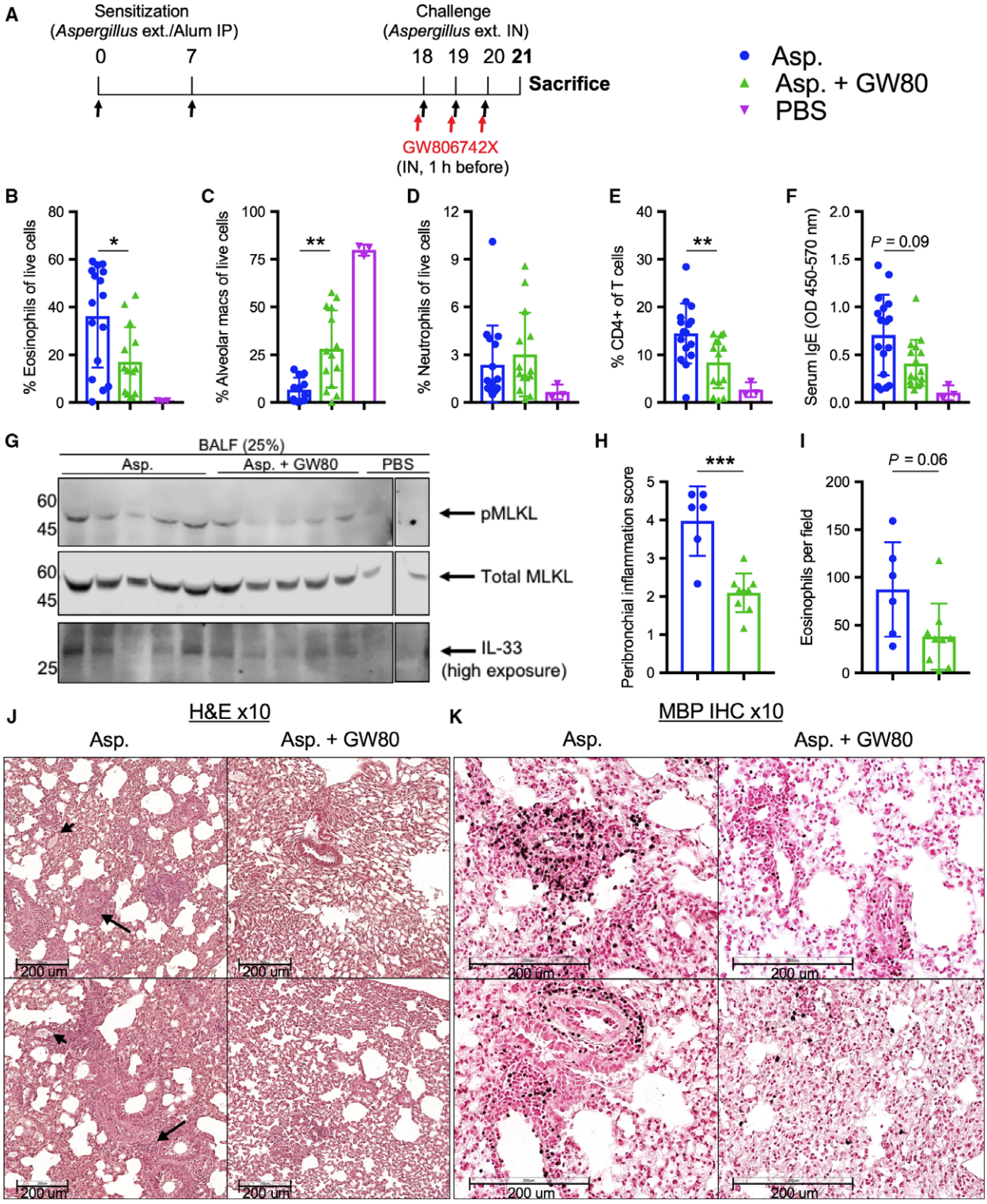

mechanism. IL-33 release from bronchial cells exposed to *A. alternata* allergenic extract was shown to be dependent on ATP-mediated Ca^{2+} increase [65]. Yet, *A. alternata* treatment was also shown to increase necrosis of naïve murine lung cells in a similar IL-33-release system, arguing that necroptosis may be responsible for its regulated release [66].

Interleukin-33 was first suspected to be a necroptotic DAMP, as mice lacking caspase-8 in keratinocytes develop an atopic dermatitis-like disease and upregulate *Il33* gene expression [67,68]. Similarly, RIPK3-induced necroptosis increased *Il33* gene expression in intestinal epithelial cells *in vitro* [69]. Nec-1s downregulates liver IL-33 protein expression in *Listeria monocytogenes*-infected mice [70], and attenuates D-Galactosamine/Lipopolysaccharide-induced hepatocellular damage and serum IL-33 [71]. However, due to its nuclear translocation sequence, IL-33 expression does not necessarily correlate with its release.

In summary, our findings that necroptotic cell death can release bioactive IL-33, and that necroptosis exacerbates allergic inflammation in an *Aspergillus*-induced asthma model (a known IL-33 disease model) underline the possibility that necroptosis facilitates inflammation in IL-33-related pathologies. Our results point to the need to study the role of MLKL, RIPK3, and RIPK1 in IL-33-related diseases, especially as pharmacological inhibitors for necroptosis enter clinical development.

Materials and methods

Reagents

Recombinant human TNFα was purchased from PeproTech (Rocky Hill, NJ, USA). The SMAC mimetics, 3,3′-[2,4-Hexadiyne-1,6-diylbis[oxy[(1S,2R)-2,3-dihydro-1H-indene-2,1 diyl]]]bis[*N*-methyl-L-alanyl-(2S)-2-cyclohexylglycyl-L-prolinamide (AZD 5582) dihydrochloride and the MLKL inhibitor, NSA, were purchased from Tocris Bioscience (Bristol, UK). The pan-caspase inhibitor, Z-VAD-fmk (zVAD), the RIPK1 inhibitor, Nec-1s, and the RIP3 inhibitor, GSK'872, were purchased from Calbiochem (Merck Millipore, Danvers, MA, USA). The necroptosis inhibitor GW80 was purchased from Sigma-Aldrich (Merck Millipore). Halt protease and the phosphatase inhibitors cocktail EDTA free was purchased from Pierce Biotechnology (Thermo Fisher Scientific, Waltham, MA, USA). Commercial antibodies were used at 1 : 1000 dilution and purchased from Abcam (Cambridge, UK; anti-human-pMLKL, 187091, and anti-mouse-pMLKL, 196436), Merck Millipore (total MLKL, MABC604), R&D systems (Minneapolis, MN, USA) (anti-mouse IL-33, AF3626), and from Cell Signaling Technology [Danvers, MA, USA; cleaved caspase-3 (CC3), 9961]. Horseradish peroxidase (HRP)-conjugated and Alexa Flour 680-conjugated Affini-Pure donkey anti-goat secondary antibodies were purchased from Jackson ImmunoResearch Labs (West Grove, PA, USA). Propidium iodide (PI) was purchased from Sigma-Aldrich (Merck Millipore).

Cell culture

The L929 murine fibrosarcoma cell line and the HaCaT human keratinocyte cell line were cultured in Dulbecco's modification of Eagle (DMEM; Biological Industries, Beit Haemek, Israel), and the KU812 human basophil cell line was cultured in Roswell Park Memorial Institute-1649 (RPMI; Biological industries), both supplemented with 10% fetal bovine serum, 1% penicillin-streptomycin, and 1% HEPES at 37 °C in a humidified 5% CO_2 atmosphere. All three reagents were purchased from Gibco (Thermo Fisher Scientific). All cell lines were tested for mycoplasma before use.

Generating of GFP- or IL-33-GFP-stably expressing cells lines

For the GFP-expressing plasmid, pLL3.7-CMV-T2A-EGFP vector was provided by the Tel Aviv University Vector Core (Tel Aviv, Israel). For the IL-33-GFP-expressing plasmid to be transduced, the cDNA for the murine IL-33 (NM_133775) was amplified from pET45b-murine IL-33 plasmid that was kindly given by Prof. Seamus Martin, using the following primers: forward, TCCGCTAGCGC CACCATGAGACCTAGAATGAAGTATTCCAACTCCA AG and reverse, TGGGGATCCGATTTTCGAGAGCT TAAACATAATATTGTTGCAGC. The insert was then restricted using Nhel and BamHI restriction enzymes (New England Biolabs, Ipswich, MA, USA), and was cloned into the restricted pLL3.7-CMV-T2A-EGFP using quick ligase (New England Biolabs) following the manufacturer's protocol, between the CMV promoter and the sequence for the T2A self-cleaving peptide. Sanger sequencing of the replaced restriction fragment was performed. Lentivirus was generated by transfecting HEK 293T cells with either pLL3.7-CMV-T2A-EGFP or pLL3.7-CMV-mIL-33-T2A-EGFP plasmids using lipofectamine 3000 reagent (Thermo Fisher Scientific) following the manufacturer's protocol. HaCaT and L929 cells were then transduced with the filtered S/N with the addition of polybrene (8 $\mu g \cdot \mu L^{-1}$). A few h later, the cells were washed and the S/N was replaced. GFP-positive cells were sorted (FACSAria, BD Biosciences, San Jose, CA, USA) 3 weeks later.

Immunofluorescence

GFP-positive-HaCaT and L929 cells were grown on coverslips and fixed for 20 min in PBS containing 4% paraformaldehyde. The coverslips were then washed for

three times and cells were permeabilized with 0.1% Triton X-100 in PBS and then blocked with 1% bovine serum albumin in the permeabilization buffer for 1 h. Next, the cells were incubated at 4 °C with polyclonal goat anti-mouse IL-33 antibody (1 : 50, AF3626, R&D). After overnight incubation, cells were incubated at room temperature with Alexa Flour 680-conjugated donkey anti-goat secondary antibody (1 : 500), for 1 h. Hoechst 33342 (1 : 1000, Calbiochem; Merck Millipore) was added for 5 min to stain cell nuclei. Cells were visualized using fluorescence microscopy (EVOS Fl Auto; Thermo Fisher Scientific).

Cell death stimuli

GFP- or IL-33-GFP-stably expressing HaCaT or L929 cells were seeded in 96-well plates (3×10^4 or 2×10^4 cells per well in 100 μL medium, respectively) for live-cell imaging, or in 24-well plates (1.5×10^5 or 1×10^5 cells per well in 500 μL medium, respectively) for subsequent western blot or ELISA analysis. On the following day, the medium was replaced with medium containing 1% FBS, supplemented with 1 $\mu g \cdot mL^{-1}$ PI and cells were treated with TNF-α (1.15 nM) and SMAC (AZD 5582, 2.5 μM; TS) to induce apoptosis, or with TNF-α, SMAC and zVAD-fmk (20 μM; TSZ) to induce necroptosis. When indicated, the necroptosis inhibitors Nec-1s (5 μM), GSK'872 (5 μM), NSA (1 μM), and GW80 (0.3 μM) were added 30 min prior to the addition of the above treatments.

To study the cell death kinetics of KU812 cells and primary IL-5 tg eosinophils, 1×10^5 cells were seeded in 200 μL DMEM per well of a 96-well plate and cells were treated with apoptotic (TS) or necroptotic (TSZ) stimuli with, or without, the addition of Nec-1s, as described above.

Live imaging assay

Plates with stimulated cells were placed on the IncucyteZOOM and 1 or 9 images per well were recorded for the 96- or 24-well plates, respectively, every 10–30 min. Data were analyzed using the IncucyteZoom2016B analysis software (Essen BioScience, Inc., Ann Arbor, MI, USA) and exported to GRAPHPAD PRISM software (GraphPad Software, San Diego, CA, USA). Normalization was then performed according to the maximal PI-positive object count to generate the frequency of dead cells.

Western blots

Stimulated cells and their S/Ns were collected at the indicated time points. S/N was first centrifuged for 5 min at 400 ***g*** to pellet cellular debris. Cells were then lysed by the addition of RIPA buffer in the presence of the HALT protease and phosphatase inhibitors cocktail for 15 min at 4 °C. S/Ns were concentrated by a methanol-chloroform protein precipitation method, as recently described [72]. Samples were mixed with SDS/PAGE loading buffer, boiled for 5 min, and loaded into SDS/PAGE precast gels (BIO-RAD, Rishon LeTsiyon, Israel) for western blot analysis. Proteins were transferred onto 0.2 μm nitrocellulose membrane using the Trans-Blot Turbo Transfer system (BIO-RAD). Membranes were blocked with 5% skim milk in TBS-T (20 mM Tris pH 7.4, 150 mM NaCl, 0.05% Tween-20) for 1 h and probed overnight with the primary antibodies, as indicated above, diluted in 5% skim milk in TBS-T, followed by washes and addition of HRP-conjugated secondary antibodies (1 : 5000 in 5% skim milk in TBS-T) for 1 h. Images were taken using Odyssey Fc system (LI-COR Biosciences, Lincoln, NE, USA) and analyzed using IMAGESTUDIO ANALYSIS software (LI-COR Biosciences).

Fractionation of supernatant proteins

Supernatants were collected at the indicated time points. S/Ns were first centrifuged for 5 min at 400 ***g*** to remove cellular debris. Protein fractions were isolated by size exclusion chromatography using the qEV commercial kit (Izon Sciences, Medford, MA, USA) according to the manufacturer's instructions. Briefly, 10 mL of S/N from stimulated cells was concentrated into 500 μL using 3KD Amicon Ultra 15 mL Centrifugal filters (Merck Millipore). Every three consecutive fractions (500 μL each) were fused and concentrated by methanol-chloroform protein precipitation method, as recently described [72] for western blot analysis. Extracellular vesicles are isolated in fractions 7–9, while free proteins are in fractions 13–25.

Primary IL-5 tg eosinophil isolation for bioactivity assay

Peritoneal lavage of CD3-IL-5 tg mice was performed by flushing the peritoneal cavity with 5 mL PBS. Peritoneal fluid was centrifuged for 5 min at 400 ***g*** and the cells were then enriched for eosinophils using negative selection with magnetic beads (Dynabeads; Invitrogen, Thermo Fisher Scientific) linked to anti-mouse pan-B (B220) and anti-mouse pan-T (CD90.2) antibodies, according to the manufacturer's instructions.

Bioactivity assay

To confirm the bioactivity system, 1×10^5 KU812 cells or primary IL-5 tg eosinophils were seeded in 200 μL DMEM per well of 96-well plates. 12.5–100 $ng \cdot mL^{-1}$ recombinant murine IL-33 (amino acids 109–266; Peprotch, Rehovot, Israel) were added, as indicated. The plates were centrifuged after 24 h and the S/N was collected to measure human IL-5 (secreted from the KU812 cells) or murine IL-6 (secreted from the primary IL-5 tg eosinophils) by ELISA.

For bioactivity assays, GFP- or IL-33-GFP-stably expressing HaCaT cells were seeded in 96-well plates (3×10^4 or per well in 100 μL medium) and were treated

with apoptotic or necroptotic stimuli on the following day, as described above. After 6 or 16 h of stimulation, 4×10^5 KU812 cells or 1×10^5 primary IL-5 tg eosinophils were added per well. The plates were centrifuged after 24 h and S/Ns were collected to measure human IL-5 (secreted from the KU812 cells) or murine IL-6 (secreted from the primary IL-5 tg eosinophils) by ELISA.

ELISA

Murine IL-33, murine IL-6, and serum mouse total IgE were measured using commercial ELISA kits obtained from Invitrogen, Thermo Fisher Scientific (Lower detection limits: 25, 4 and 4 $ng{\cdot}mL^{-1}$, respectively), according to manufacturer's protocol. Human IL-5 was assessed using ELISA MAX Standard (Biolegend, San Diego, CA, USA, Lower detection limit: 7.81 $pg{\cdot}mL^{-1}$), according to the manufacturer's protocol.

Mice

Female 6–7-week-old C57BL/6J-RccHsd mice were obtained from Envigo RMS (Jerusalem, Israel). CD3-IL-5-transgenic (NJ.1638, $Il5^{Tg}$) mice were kindly provided by J. Lee (Mayo Clinic, Scottsdale, AZ, USA) and grown in-house. All experiments were reviewed and approved by the Animal Care Committee of Tel Aviv University (Number 01-16-094) and were performed according to its regulations and guidelines regarding the care and use of animals for experimental procedures. All experiments were conducted in the specific pathogen-free facility of Tel Aviv University.

Allergen sensitization and challenge

Asthma was induced by sensitizing mice by IP of 20 μg of *Asp*. (Greer Laboratories, Lenoir, NC, USA) in 200 μL saline containing Alum (Imject Alum Adjuvant, 77161, Thermo Scientific) in a 1 : 1 ratio on days 0 and 7, using a 25 G needle. The sensitization mix was mixed for 30 min prior to use to ensure efficient antigen absorption by the Alum particles. For challenge, on days 18, 19, and 20, mice were anesthetized by isoflurane inhalation, and 10 μg *Asp*. in 50 μL of saline was applied to the nasal cavity using a micropipette while the mice were held in the supine position. Mice were held upright for 5 s after each administration. Where indicated, GW80, a necroptosis inhibitor (100 μM in 50 μL saline) was also given intranasally 1 h prior to challenge. Mice were bled and killed 24 h after the last challenge, and BAL was performed by washing the lungs three times with 500 μL saline. Following centrifugation, cells were assessed by flow cytometry.

Flow cytometry

Flow cytometric analysis of BAL cells was conducted using the following antibodies: anti-CD4 (RM-4; Biogems, PeproTech, Rehovot, Israel, 1 : 300), anti-B220 (RA3-6B2; Biogems, 1 : 300), anti-CD8 (2.43; Biogems, 1 : 300), anti-Ly6G (1A8; Biogems, 1 : 200), anti-CD11b (M1/70; Biogems, 1 : 300), anti-Ly6C (HK1.4; Biolegend, 1 : 200), anti-CD11c (N418; Invitrogen, 1 : 100), anti-SiglecF (E50-2440; BD Horizon, BD Biosciences, 1 : 200). PI (1 $\mu g{\cdot}mL^{-1}$) was used for dead cells exclusion. Samples were acquired by the flow cytometry Attune NxT (Thermo Fisher Scientific) and data were analyzed using FLOWJO (TreeStar, Ashland, OR, USA) software to study eosinophils ($CD11c^-$, $Ly6G^-$, $Cd11b^+$, $SiglecF^+$), alveolar macrophages ($CD11c^+$, $Ly6G^-$, $Cd11b^-$, $SiglecF^+$), neutrophils ($CD11c^-$, $Ly6G^+$, $Cd11b^+$, $Ly6C^+$), $CD8^+$ T cells ($CD11c^-$, $Ly6G^-$, $Cd11b^-$, $SiglecF^-$, $B220^-$, $CD8^+$), and $CD4^+$ T cells ($CD11c^-$, $Ly6G^-$, $Cd11b^-$, $SiglecF^-$, $B220^-$, $CD4^+$).

Histology and immunohistochemistry

The left lung was fixed in 4% paraformaldehyde in PBS, embedded in paraffin, and cut into 5-μm sections. Sections were deparaffinized and stained with hematoxylin and eosin (H&E). The inflammatory state of the lungs was evaluated by two independent researchers by 1–5 scoring of cellular infiltration at 1× magnification and peribronchial inflammation (assessed by peribronchial infiltration and mucus accumulation) at 10× magnification. Some of the sections were deparaffinized and immunostained with anti-major basic protein (anti-MBP) antibody (from J. Lee's, Mayo clinic) by the common immunohistochemistry procedure [73]. Eosinophils (MBP- labeled cells) were acquired and counted using IMAGEJ (National Institutes of Health, Bethesda, MD, USA).

Statistical analysis

Statistical analysis was performed using GRAPHPAD PRISM 7 software.

Acknowledgements

This work was performed in partial fulfillment of the requirements for a PhD degree (IS), Sackler Faculty of Medicine, Tel Aviv University, Israel. We thank Prof. Jean-Philippe Girard and Dr. Corrine Cayrol for generously advising and sharing the KU812 cell line. We would also like to thank Prof. Seamus Martin for generously provision of pET45b-murine IL-33 plasmid. We thank Sharon Grisaru and Ophir Shani for their assistance with histology. The research of MG was supported by the Israel Science Foundation (ISF) (grant #1416/15 & 818/18), Alpha-1 Foundation and the United States – Israel Binational Science Foundation (BSF) (grant #2017176). The research of BC was supported by the NIH grant 5RO1HL124209, the

American Asthma Foundation and BSF (grant #2017176). IS has been supported by the Naomi Foundation through the Tel Aviv University GRTF Program.

Conflict of interest

The authors declare no conflicts of interest.

Authors' contributions

Conceptualization: IS, MG. Funding acquisition: BC, MG. Investigation: IS, ZE, MS, SZ, NB, ME, LEB, MG. Methodology: IS, MS, LEB, AM, MG. Supervision: LE, MG. Validation: ME. Writing – original draft: IS, MG. Writing – review & editing: MS, AM, BC.

References

1 Schmitz J, Owyang A, Oldham E, Song Y, Murphy E, McClanahan TK, Zurawski G, Moshrefi M, Qin J, Li X *et al.* (2005) IL-33, an interleukin-1-like cytokine that signals via the IL-1 receptor-related protein ST2 and induces T helper type 2-associated cytokines. *Immunity* **23**, 479–490.

2 Moussion C, Ortega N & Girard JP (2008) The IL-1-like cytokine IL-33 is constitutively expressed in the nucleus of endothelial cells and epithelial cells *in vivo*: a novel "Alarmin"? *PLoS ONE* **3**, 1–8.

3 Pichery M, Mirey E, Mercier P, Lefrancais E, Dujardin A, Ortega N & Girard J-P (2012) Endogenous IL-33 Is highly expressed in mouse epithelial barrier tissues, lymphoid organs, brain, embryos, and inflamed tissues. *In situ* analysis using a novel Il-33-LacZ gene trap reporter strain. *J Immunol* **188**, 3488–3495.

4 Roussel L, Erard M, Cayrol C & Girard JP (2008) Molecular mimicry between IL-33 and KSHV for attachment to chromatin through the H2A-H2B acidic pocket. *EMBO Rep* **9**, 1006–1012.

5 Travers J, Rochman M, Miracle CE, Habel JE, Caldwell JM, Rymer JK, Rothenberg ME & Brusilovsky M (2018) Chromatin regulates IL-33 release and extracellular cytokine activity. *Nat Commun* **9**, 1–15.

6 Lott JM, Sumpter TL & Turnquist HR (2015) New dog and new tricks: evolving roles for IL-33 in type 2 immunity. *J Leukoc Biol* **97**, 1037–1048.

7 Bessa J, Meyer CA, de Vera Mudry MC, Schlicht S, Smith SH, Iglesias A & Cote-Sierra J (2015) Altered subcellular localization of IL-33 leads to non-resolving lethal inflammation. *J Autoimmun* **55**, 33–41.

8 Luthi AU, Cullen SP, McNeela EA, Duriez PJ, Afonina IS, Sheridan C, Brumatti G, Taylor RC, Kersse K, Vandenabeele P *et al.* (2009) Suppression of interleukin-33 bioactivity through proteolysis by apoptotic caspases. *Immunity* **31**, 84–98.

9 Cayrol C & Girard J-P (2009) The IL-1-like cytokine IL-33 is inactivated after maturation by caspase-1. *Proc Natl Acad Sci* **106**, 9021–9026.

10 Lefrançais E, Roga S, Gautier V, Gonzalez-de-Peredo A, Monsarrat B, Girard J-P & Cayrol C (2012) IL-33 is processed into mature bioactive forms by neutrophil elastase and cathepsin G. *Proc Natl Acad Sci USA* **109**, 1673–1678.

11 Lefrancais E, Duval A, Mirey E, Roga S, Espinosa E, Cayrol C & Girard JP (2014) Central domain of IL-33 is cleaved by mast cell proteases for potent activation of group-2 innate lymphoid cells. *Proc Natl Acad Sci USA* **111**, 15502–15507.

12 Clancy DM, Sullivan GP, Moran HBT, Henry CM, Reeves EP, McElvaney NG, Lavelle EC & Martin SJ (2018) Extracellular neutrophil proteases are efficient regulators of IL-1, IL-33, and IL-36 cytokine activity but poor effectors of microbial killing. *Cell Rep* **22**, 2809–2817.

13 Cayrol C, Duval A, Schmitt P, Roga S, Camus M, Stella A, Burlet-Schiltz O, Gonzalez-De-Peredo A & Girard JP (2018) Environmental allergens induce allergic inflammation through proteolytic maturation of IL-33. *Nat Immunol* **19**, 375–385.

14 Cohen ES, Scott IC, Majithiya JB, Rapley L, Kemp BP, England E, Rees DG, Overed-Sayer CL, Woods J, Bond NJ *et al.* (2015) Oxidation of the alarmin IL-33 regulates ST2-dependent inflammation. *Nat Commun* **6**, 1–10.

15 Sanada S, Hakuno D, Higgins LJ, Schreiter ER, McKenzie ANJ & Lee RT (2007) IL-33 and ST2 comprise a critical biomechanically induced and cardioprotective signaling system. *J Clin Invest* **117**, 1538–1549.

16 Prefontaine D, Lajoie-Kadoch S, Foley S, Audusseau S, Olivenstein R, Halayko AJ, Lemiere C, Martin JG & Hamid Q (2009) Increased expression of IL-33 in severe asthma: evidence of expression by airway smooth muscle cells. *J Immunol* **183**, 5094–5103.

17 Hamzaoui A, Berraies A, Kaabachi W, Haifa M, Ammar J & Kamel H (2013) Induced sputum levels of IL-33 and soluble ST2 in young asthmatic children. *J Asthma* **50**, 803–809.

18 Byers DE, Alexander-Brett J, Patel AC, Agapov E, Dang-Vu G, Jin X, Wu K, You Y, Alevy Y, Girard JP *et al.* (2013) Long-term IL-33-producing epithelial progenitor cells in chronic obstructive lung disease. *J Clin Invest* **123**, 3967–3982.

19 Moffatt MF, Gut IG, Demenais F, Strachan DP, Bouzigon E, Heath S, von Mutius E, Farrall M, Lathrop M, Cookson W; GABRIEL Consortium (2010) A large-scale, consortium-based genomewide association study of asthma. *N Engl J Med* **363**, 1211–1221.

20 Kurowska-Stolarska M, Stolarski B, Kewin P, Murphy G, Corrigan CJ, Ying S, Pitman N, Mirchandani A, Rana B, van Rooijen N *et al.* (2009) IL-33 amplifies the

polarization of alternatively activated macrophages that contribute to airway inflammation. *J Immunol* **183**, 6469–6477.
21 Baumann C, Bonilla WV, Fröhlich A, Helmstetter C, Peine M, Hegazy AN, Pinschewer DD & Löhning M (2015) T-bet– and STAT4–dependent IL-33 receptor expression directly promotes antiviral Th1 cell responses. *Proc Natl Acad Sci* **112**, 4056–4061.
22 Stolarski B, Kurowska-Stolarska M, Kewin P, Xu D & Liew FY (2010) IL-33 exacerbates eosinophil-mediated airway inflammation. *J Immunol* **185**, 3472–3480.
23 Kondo Y, Yoshimoto T, Yasuda K, Futatsugi-yumikura S, Morimoto M, Hayashi N, Hoshino T, Fujimoto J & Nakanishi K (2008) Administration of IL-33 induces airway hyperresponsiveness and goblet cell hyperplasia in the lungs in the absence of adaptive immune system. *Int Immunol* **20**, 791–800.
24 Matsuyama Y, Okazaki H, Tamemoto H, Kimura H, Kamata Y, Nagatani K, Nagashima T, Hayakawa M, Iwamoto M, YOSHIO T *et al.* (2010) Increased levels of interleukin 33 in sera and synovial fluid from patients with active rheumatoid arthritis. *J Rheumatol* **37**, 18–25.
25 Rose WA, Okragly AJ, Patel CN & Benschop RJ (2015) IL-33 released by alum is responsible for early cytokine production and has adjuvant properties. *Sci Rep* **5**, 1–13.
26 Kakkar R, Hei H, Dobner S & Lee RT (2012) Interleukin 33 as a mechanically responsive cytokine secreted by living cells. *J Biol Chem* **287**, 6941–6948.
27 Holler N, Zaru R, Micheau O, Thome M, Attinger A, Valitutti S, Bodmer JL, Schneider P, Seed B & Tschopp J (2000) Fas triggers an alternative, caspase-8-independent cell death pathway using the kinase RIP as effector molecule. *Nat Immunol* **1**, 489–495.
28 He S, Wang L, Miao L, Wang T, Du F, Zhao L & Wang X (2009) Receptor interacting protein kinase-3 determines cellular necrotic response to TNF-α. *Cell* **137**, 1100–1111.
29 He S, Liang Y, Shao F & Wang X (2011) Toll-like receptors activate programmed necrosis in macrophages through a receptor-interacting kinase-3-mediated pathway. *Proc Natl Acad Sci* **108**, 20054–20059.
30 Kaiser WJ, Sridharan H, Huang C, Mandal P, Upton JW, Gough PJ, Sehon CA, Marquis RW, Bertin J & Mocarski ES (2013) Toll-like receptor 3-mediated necrosis via TRIF, RIP3, and MLKL. *J Biol Chem* **288**, 31268–31279.
31 Silke J, Rickard JA & Gerlic M (2015) The diverse role of RIP kinases in necroptosis and inflammation. *Nat Immunol* **16**, 689–697.
32 Oberst A, Dillon CP, Weinlich R, McCormick LL, Fitzgerald P, Pop C, Hakem R, Salvesen GS & Green DR (2011) Catalytic activity of the caspase-8-FLIP L complex inhibits RIPK3-dependent necrosis. *Nature* **471**, 363–368.
33 Kaiser WJ, Upton JW, Long AB, Livingston-Rosanoff D, Daley-Bauer LP, Hakem R, Caspary T & Mocarski ES (2011) RIP3 mediates the embryonic lethality of caspase-8-deficient mice. *Nature* **471**, 368–372.
34 Shlomovitz I, Zargrian S & Gerlic M (2017) Mechanisms of RIPK3-induced inflammation. *Immunol Cell Biol* **95**, 166–172.
35 Cho YS, Challa S, Moquin D, Genga R, Ray TD, Guildford M & Chan FKM (2009) Phosphorylation-driven assembly of the RIP1-RIP3 complex regulates programmed necrosis and virus-induced inflammation. *Cell* **137**, 1112–1123.
36 Murphy JM, Czabotar PE, Hildebrand JM, Lucet IS, Zhang JG, Alvarez-Diaz S, Lewis R, Lalaoui N, Metcalf D, Webb AI *et al.* (2013) The pseudokinase MLKL mediates necroptosis via a molecular switch mechanism. *Immunity* **39**, 443–453.
37 Sun L, Wang H, Wang Z, He S, Chen S, Liao D, Wang L, Yan J, Liu W, Lei X *et al.* (2012) Mixed lineage kinase domain-like protein mediates necrosis signaling downstream of RIP3 kinase. *Cell* **148**, 213–227.
38 Hildebrand JM, Tanzer MC, Lucet IS, Young SN, Spall SK, Sharma P, Pierotti C, Garnier J-M, Dobson RCJ, Webb AI *et al.* (2014) Activation of the pseudokinase MLKL unleashes the four-helix bundle domain to induce membrane localization and necroptotic cell death. *Proc Natl Acad Sci* **111**, 15072–15077.
39 Dondelinger Y, Declercq W, Montessuit S, Roelandt R, Goncalves A, Bruggeman I, Hulpiau P, Weber K, Sehon CA, Marquis RW *et al.* (2014) MLKL compromises plasma membrane integrity by binding to phosphatidylinositol phosphates. *Cell Rep* **7**, 971–981.
40 Cai Z, Jitkaew S, Zhao J, Chiang HC, Choksi S, Liu J, Ward Y, Wu LG & Liu ZG (2014) Plasma membrane translocation of trimerized MLKL protein is required for TNF-induced necroptosis. *Nat Cell Biol* **16**, 55–65.
41 Degterev A, Huang Z, Boyce M, Li Y, Jagtap P, Mizushima N, Cuny GD, Mitchison TJ, Moskowitz MA & Yuan J (2005) Chemical inhibitor of nonapoptotic cell death with therapeutic potential for ischemic brain injury. *Nat Chem Biol* **1**, 112–119.
42 Degterev A, Hitomi J, Germscheid M, Ch'en IL, Korkina O, Teng X, Abbott D, Cuny GD, Yuan C, Wagner G *et al.* (2008) Identification of RIP1 kinase as a specific cellular target of necrostatins. *Nat Chem Biol* **4**, 313–321.
43 Yan B, Liu L, Huang S, Ren Y, Wang H, Yao Z, Li L, Chen S, Wang X & Zhang Z (2017) Discovery of a new class of highly potent necroptosis inhibitors targeting the mixed lineage kinase domain-like protein. *Chem Commun* **53**, 3637–3640.

44 Rickard JA, O'Donnell JA, Evans JM, Lalaoui N, Poh AR, Rogers T, Vince JE, Lawlor KE, Ninnis RL, Anderton H *et al.* (2014) RIPK1 regulates RIPK3-MLKL-driven systemic inflammation and emergency hematopoiesis. *Cell* **157**, 1175–1188.
45 Pasparakis M & Vandenabeele P (2015) Necroptosis and its role in inflammation. *Nature* **517**, 311–320.
46 Kaczmarek A, Vandenabeele P & Krysko DV (2013) Necroptosis: the release of damage-associated molecular patterns and its physiological relevance. *Immunity* **38**, 209–223.
47 Carriere V, Roussel L, Ortega N, Lacorre DA, Americh L, Aguilar L, Bouche G & Girard JP (2007) IL-33, the IL-1-like cytokine ligand for ST2 receptor, is a chromatin-associated nuclear factor *in vivo*. *Proc Natl Acad Sci USA* **104**, 282–287.
48 Zargarian S, Shlomovitz I, Erlich Z, Hourizadeh A, Ofir-Birin Y, Croker BA, Regev-Rudzki N, Edry-Botzer L & Gerlic M (2017) Phosphatidylserine externalization, "necroptotic bodies" release, and phagocytosis during necroptosis. *PLoS Biol* **15**, 1– 23.
49 Denecker G, Vercammen D, Steemans M, Vanden Berghe T, Brouckaert G, Van Loo G, Zhivotovsky B, Fiers W, Grooten J, Declercq W *et al.* (2001) Death receptor-induced apoptotic and necrotic cell death: differential role of caspases and mitochondria. *Cell Death Differ* **8**, 829–840.
50 Shik D, Moshkovits I, Karo-Atar D, Reichman H & Munitz A (2014) Interleukin-33 requires CMRF35-like molecule-1 expression for induction of myeloid cell activation. *Allergy* **69**, 719–729.
51 Masaki K, Fukunaga K, Matsusaka M, Kabata H, Tanosaki T, Mochimaru T, Kamatani T, Ohtsuka K, Baba R, Ueda S *et al.* (2017) Characteristics of severe asthma with fungal sensitization. *Ann Allergy Asthma Immunol* **119**, 253–257.
52 Denning DW, O'Driscoll BR, Hogaboam CM, Bowyer P & Niven RM (2006) The link between fungi and severe asthma: a summary of the evidence. *Eur Respir J* **27**, 615–626.
53 Castanhinha S, Sherburn R, Walker S, Gupta A, Bossley CJ, Buckley J, Ullmann N, Grychtol R, Campbell G, Maglione M *et al.* (2015) Pediatric severe asthma with fungal sensitization is mediated by steroid-resistant IL-33. *J Allergy Clin Immunol* **136**, 312–322.e7.
54 Ramaprakash H, Shibata T, Duffy KE, Ismailoglu UB, Bredernitz RM, Moreira AP, Coelho AL, Das AM, Fursov N, Chupp GL *et al.* (2011) Targeting ST2L potentiates CpG-mediated therapeutic effects in a chronic fungal asthma model. *Am J Pathol* **179**, 104–115.
55 Albacker LA, Chaudhary V, Chang Y-J, Kim HY, Chuang Y-T, Pichavant M, DeKruyff RH, Savage PB & Umetsu DT (2013) Invariant natural killer T cells recognize a fungal glycosphingolipid that can induce airway hyperreactivity. *Nat Med* **19**, 1297–1304.
56 Wang X, He Z, Liu H, Yousefi S & Simon H-U (2016) Neutrophil necroptosis is triggered by ligation of adhesion molecules following GM-CSF priming. *J Immunol* **197**, 4090–4100.
57 González-Juarbe N, Gilley RP, Hinojosa CA, Bradley KM, Kamei A, Gao G, Dube PH, Bergman MA & Orihuela CJ (2015) Pore-forming toxins induce macrophage necroptosis during acute bacterial pneumonia. *PLoS Pathog* **11**, 1–23.
58 Liew FY, Girard JP & Turnquist HR (2016) Interleukin-33 in health and disease. *Nat Rev Immunol* **16**, 676–689.
59 Bertheloot D & Latz E (2017) HMGB1, IL-1α, IL-33 and S100 proteins: dual-function alarmins. *Cell Mol Immunol* **14**, 43–64.
60 Martin SJ (2016) Cell death and inflammation: the case for IL-1 family cytokines as the canonical DAMPs of the immune system. *FEBS J* **283**, 2599–2615.
61 Baekkevold ES & Roussigne M (2003) Molecular characterization of NF-HEV, a nuclear factor preferentially expressed in human high endothelial venules. *Am J Pathol* **163**, 69–79.
62 Liu X, Hammel M, He Y, Tainer JA, Jeng U-S, Zhang L, Wang S & Wang X (2013) Structural insights into the interaction of IL-33 with its receptors. *Proc Natl Acad Sci* **110**, 14918–14923.
63 Zhang L, Lu R, Zhao G, Pflugfelder SC & Li DQ (2011) TLR-mediated induction of pro-allergic cytokine IL-33 in ocular mucosal epithelium. *Int J Biochem Cell Biol* **43**, 1383–1391.
64 Hudson CA, Christophi GP, Gruber RC, Wilmore JR, Lawrence DA & Massa PT (2008) Induction of IL-33 expression and activity in central nervous system glia. *J Leukoc Biol* **84**, 631–643.
65 Kouzaki H, Iijima K, Kobayashi T, O'Grady SM & Kita H (2011) The danger signal, extracellular ATP, is a sensor for an airborne allergen and triggers IL-33 release and innate Th2-type responses. *J Immunol* **186**, 4375–4387.
66 Osbourne MM (2017) HpARI protein secreted by a helminth parasite suppresses interleukin-33. *Immunity* **47**, 739–751.
67 Li C, Lasse S, Lee P, Nakasaki M, Chen SW, Yamasaki K, Gallo RL & Jamora C (2010) Development of atopic dermatitis-like skin disease from the chronic loss of epidermal caspase-8. *Proc Natl Acad Sci USA* **107**, 22249–22254.
68 Kovalenko A, Kim JC, Kang TB, Rajput A, Bogdanov K, Dittrich-Breiholz O, Kracht M, Brenner O & Wallach D (2009) Caspase-8 deficiency in epidermal keratinocytes triggers an inflammatory skin disease. *J Exp Med* **206**, 2161–2177.
69 Negroni A, Colantoni E, Pierdomenico M, Palone F, Costanzo M, Oliva S, Tiberti A, Cucchiara S & Stronati L (2017) RIP3 AND pMLKL promote

necroptosis-induced inflammation and alter membrane permeability in intestinal epithelial cells. *Dig Liver Dis* **49**, 1201–1210.

70 Blériot C, Dupuis T, Jouvion G, Eberl G, Disson O & Lecuit M (2015) Liver-resident macrophage necroptosis orchestrates type 1 microbicidal inflammation and type-2-mediated tissue repair during bacterial infection. *Immunity* **42**, 145–158.

71 Seo MJ, Hong JM, Kim SJ & Lee SM (2017) Genipin protects D-galactosamine and lipopolysaccharide-induced hepatic injury through suppression of the necroptosis-mediated inflammasome signaling. *Eur J Pharmacol* **812**, 128–137.

72 Shlomovitz I, Zargarian S, Erlich Z & Edry-botzer L (2018) Distinguishing necroptosis from apoptosis. In Programmed Necropsis. Methods in Molecular Biology, Vol. 1857 (Ting A, ed), pp. 35–51. Humana Press, New York, NY.

73 Denzler KL, Farmer SC, Crosby JR, Borchers M, Cieslewicz G, Larson KA, Cormier-Regard S, Lee NA & Lee JJ (2000) Eosinophil major basic protein-1 does not contribute to allergen-induced airway pathologies in mouse models of asthma. *J Immunol* **165**, 5509–5517.